

Growth and division mode plasticity is dependent on cell density in marine-derived black yeasts

Gohta Goshima^{1,2}

¹ Sugashima Marine Biological Laboratory, Graduate School of Science, Nagoya University, Sugashima, 429-63, Toba 517-0004, Japan

² Division of Biological Science, Graduate School of Science, Nagoya University, Furocho, Chikusa-ku, Nagoya 464-8602, Japan

Email: goshima@bio.nagoya-u.ac.jp

Phone: +81 599-34-2216

Abstract

The diversity and ecological contribution of the fungus kingdom in the marine environment remain under-studied. A recent survey in the Atlantic (Woods Hole, MA, USA) brought to light the diversity and unique biological features of marine fungi. The study revealed that black yeast species undergo an unconventional cell division cycle, which has not been documented in conventional model yeast species such as *Saccharomyces cerevisiae* (budding yeast) and *Schizosaccharomyces pombe* (fission yeast). The prevalence of this unusual property is unknown. Here, I collected and identified 65 marine fungi species across 40 genera from the surface ocean water, sediment, and the surface of macroalgae (seaweeds) in the Pacific (Sugashima, Toba, Japan). The Sugashima collection largely did not overlap with the Woods Hole collection and included several unidentifiable species, further illustrating the diversity of marine fungi. Three black yeast species were isolated, two of which were commonly found in Woods Hole (*Aureobasidium pullulans*, *Hortaea werneckii*). Surprisingly, their cell division mode was dependent on cell density, and the previously reported unconventional division mode was reproduced only at a certain cell density. For all three black yeast species, cells underwent filamentous growth with septations at low cell density and immediately formed buds at high cell density. At intermediate cell density, two black yeasts (*H. werneckii* and an unidentifiable species) showed rod cells undergoing septation at the cell equator. In contrast, all eight budding yeast species showed a consistent division pattern regardless of cell density. This study suggests the plastic nature of the growth/division mode of marine-derived black yeast.

Introduction

Understanding the habitats of marine organisms is important for understanding marine ecology. Much of this effort has been put on macro-organisms, such as fishes and benthic invertebrates, as well as unicellular microorganisms such as algae and bacteria (OBIS, <https://obis.org/>). Relatively little attention has been paid to fungi, and little is known about their life cycle and physiology (Amend et al., 2019; Gladfelter et al., 2019). The genetics and cell biology of these organisms have been pioneered in a few terrestrial fungal systems, such as *Saccharomyces cerevisiae*, *Schizosaccharomyces pombe*, and *Aspergillus nidulans* (Feyder et al., 2015; Nurse and Hayles, 2019; Osmani and Mirabito,

46 2004). An important step towards understanding the ecology of marine fungi is the
47 identification of fungi in various locations.

48 An interesting study was published in 2019, in which 35 fungi were collected from
49 the sediment, surface ocean water, and benthic animals (corals, sponges) around Woods
50 Hole, MA, USA (Mitchison-Field et al., 2019). That study investigated the division
51 pattern of several black yeast species, which is a polyphyletic group of fungi that has
52 melanised cell walls. Black yeasts have been of ecological interest, as they are tolerant to
53 extreme environmental conditions such as super-high salinity (Gostincar et al., 2012;
54 Moreno et al., 2018). Live imaging of black yeasts uncovered remarkable unconventional
55 features in their cell division cycle (Mitchison-Field et al., 2019). For example, a single
56 *Hortaea werneckii* cell always underwent fission during its first cell division, but the next
57 division involved budding at 92% probability. This observation challenged the
58 conventional view that a single cell division pattern is intrinsic to a yeast species; for
59 example, *S. pombe* and *S. cerevisiae* always divide via fission or budding, respectively.
60 In another striking example, more than 50% of *Aureobasidium pullulans* cells produced
61 multiple rounds of simultaneous buds, which is never observed in *S. cerevisiae*
62 (Mitchison-Field et al., 2019). From an ecological point of view, this study urges the
63 necessity of further sampling and characterisation, as what has been reported to date is
64 unlikely to be the full set of marine fungi in the ocean.

65 In this study, inspired by (Mitchison-Field et al., 2019), free-living marine fungi were
66 collected in front of Nagoya University's Marine Biological Laboratory (NU-MBL) on
67 Sugashima Island, Toba, Japan (Fig. 1A). The species were identified via DNA barcode
68 sequencing, and the division pattern was observed for budding and black yeasts (no
69 fission yeast was isolated). The collected species, or even genera, only partially
70 overlapped with those identified by (Mitchison-Field et al., 2019), suggesting the
71 existence of highly divergent fungal species in the ocean. Surprisingly, the division
72 pattern of black yeasts (*H. werneckii*, *A. pullulans*, and other unidentified species) was
73 initially inconsistent with those previously reported in (Mitchison-Field et al., 2019), and
74 this enigma was solved through the observation of cell density-dependent alterations in
75 their division patterns.

76

77 **Results**

78

79 **Isolation of fungi at the Sugashima marine laboratory**

80 Fungi were isolated from four sources: surface ocean sea water near the beach (Fig. 1B,
81 green), an outdoor tank that has various benthic animals and seaweeds (circulated surface
82 water and sediment; Fig. 1C), and sliced seaweeds (each ~3 cm) that were collected in
83 the intertidal zone in front of the laboratory (Fig. 1B [magenta], D). The sediment was
84 most enriched with fungi (Fig. 1E; 200 μ L sediment). Fungal colonies were obtained from
85 100 mL surface sea water, and 7.5 ± 8.5 fungal colonies were obtained ($n = 6$), whereas
86 seaweeds were a more abundant source of fungi (25 ± 26 colonies isolated from a ~3 cm
87 piece of seaweed body [$n = 10$]). However, based on colony colour and shape, it was
88 deduced that many colonies were derived from the same species. In total, 74 colonies
89 were regrown on separate plates (15 examples are shown in Fig. 2), and two (ITS1/4 and
90 NL1/4) or more barcode regions were sequenced (Table 1, Table S1). For some clones,
91 the species or even genera could not be identified because of the high deviation of the
92 barcode sequences from the known sequences registered in the database (named with "sp."

93 or described as “unclear” in Table 2). The total number of species collected was 65 (Table
94 2).

95

96 **Comparison with the Woods Hole collection**

97 There were considerable differences between the current collection at Sugashima and
98 what was identified around Woods Hole (Mitchison-Field et al., 2019) (Table 2, *1). Only
99 seven species were isolated in both studies (*Aureobasidium pullulans*, *Cladosporium*
100 *cladosporioides*, *Cladosporium halotolerans*, *Hortaea werneckii*, *Metschnikowia*
101 *bicuspidate*, *Meyerozyma guilliermondii*, and *Parengyodontium album*). At the genus
102 level, only 13 genera were common (*Aspergillus*, *Candida*, *Epicoccum*, *Filobasidium*,
103 *Penicillium*, *Rhodotorula*, and *Trichoderma*, in addition to aforementioned six genera),
104 while other genera were uniquely isolated in either location: 27 from Sugashima
105 (*Alternaria*, *Arthopyrenia*, *Arthrimum*, *Cystobasidium*, *Diaporthe*, *Didymella*, *Fusarium*,
106 *Kluyveromyces*, *Letendreaa*, *Leucosporidium*, *Microdochium*, *Neoascochyta*,
107 *Neopestalotiopsis*, *Paraboeremia*, *Paradendryphiella*, *Pestalotiopsis*, *Phacidium*, *Phoma*,
108 *Pyrenochaetopsis*, *Simplicillium*, *Sphaerulina*, *Umbelopsis*, *Ustilago*, and four unclear
109 genera), and six from Woods Hole (*Apiotrichum*, *Cadophora*, *Cryptococcus*, *Exophiala*,
110 *Knufia*, *Phaeotheca*). While this discrepancy may partly stem from seasonal or regional
111 differences, it more likely reflects the limited coverage of fungi in both studies. The
112 current survey agrees with the view that many more species exist in the ocean (Amend et
113 al., 2019).

114

115 **Budding yeast species with fixed and variable bud positions**

116 Fifteen fungal species produced yeast-like colonies on culture plates. Live imaging was
117 performed for these species at least thrice at different cell densities. Five of them turned
118 out to have *S. cerevisiae*-like budding-growth cycles, where a daughter cell emerged from
119 the round-shaped mother cell and a mother cell can produce a second daughter at other
120 sites than the previous one (*Candida sake*, *Kluyveromyces nonfermentans*,
121 *Metschnikowia bicuspidate*, *Meyerozyma guilliermondii*, *Rhodotorula* sp.) (Fig. 3A,
122 Video 1). Interestingly, the budding sites of three other yeasts were fixed, although the
123 mother cell had a nearly round shape (*Cystobasidium slooffiae*, *Filobasidium magnum*,
124 *Filobasidium* sp.) (Fig. 3B, Video 1). Four other fungi were rod-shaped, in which budding
125 and/or filamentous growth were observed (*Leucosporidium intermedium*, *Ustilago* sp.,
126 *Sphaerulina rhabdoclinis*, *Sphaerulina* sp.) (Video 2).

127

128 **Cell density-dependent division pattern alteration in the black yeast *A. pullulans***

129 The remaining three fungi that formed yeast-like colonies produced black or brown
130 pigment. Two of them have been extensively studied by (Mitchison-Field et al., 2019): *A.*
131 *pullulans* (Fig. 4A) and *H. werneckii* (Fig. 5A). *A. pullulans* in (Mitchison-Field et al.,
132 2019) had a round shape and showed multiple buds at one site. However, in my first few
133 imaging attempts, such a characteristic division pattern was never observed. Instead, they
134 first grew as filaments, and later produced multiple buds from many locations on the
135 filament. In the course of repetitive imaging, it was noticed that a division pattern closer
136 to that described in (Mitchison-Field et al., 2019) could be obtained when the initial cell
137 density was increased. To test the possibility that the division pattern is density-dependent,
138 a 10-fold dilution series of the strain was prepared for imaging (relative cell densities: $\times 1$,
139 $\times 10$, $\times 100$, and $\times 1000$). When the initial cell density was low, a single cell first elongated

140 with occasional septation, followed by multiple budding from the elongated cell filament
141 (100%, n = 65) (Fig. 4B, D, Video 3). The higher the cell density, the faster the bud
142 emerged (Fig. 4C). Immediate budding without extensive mother cell elongation or
143 septation was observed only when the initial cell density was high (Fig. 4B, 19 out of 30
144 cells). However, the majority of the cells (14/19) showed buds at both poles of the mother
145 cell (Fig. 4E) rather than produced buds from the same pole, as reported in (Mitchison-
146 Field et al., 2019) (5/19) (Fig. 4F). Thus, this black yeast species showed division pattern
147 variation depending on the cell density.

148 An earlier study involving immunofluorescence microscopy of microtubules and
149 actin of other *A. pullulans* strains also showed filamentous morphology (Kopecka et al.,
150 2003). Therefore, time-lapse imaging of *A. pullulans* strain collected in (Mitchison-Field
151 et al., 2019) was performed in an identical condition to that for the Sugashima strain.
152 Interestingly, the Woods Hole strain also showed filamentous growth at low density
153 (100%, n = 30) and immediate multi-budding was observed only at the highest density.
154 These results suggest that density-dependency of growth/division mode alteration is a
155 common feature of *A. pullulans*.

156 **Cell density-dependent division pattern alteration in the black yeast *H. werneckii***

157 Two clones of *H. werneckii* were isolated, and their colony sizes were slightly different
158 (Fig. 5A). The barcode sequences had high similarity but were not identical (1 bp
159 mismatch). These were interpreted as natural variants of the same species. Imaging of
160 these clones initially produced puzzling results: the reported characteristic division
161 pattern— a single cell almost always undergoes fission, followed by budding (Mitchison-
162 Field et al., 2019) – was rarely observed. To test the possibility that, similar to *A. basidium*,
163 the initial cell density might have affected the division pattern, the number of inoculated
164 cells was varied ($\times 1$, $\times 10$, $\times 100$, $\times 300$). The initial cell numbers dramatically affected the
165 mode of the first few cell divisions in both isolates (Fig. 5B presents the result of NU28;
166 Video 4). Multiple rounds of septation were observed when cell density was low and
167 multiple budding occurred hours later (Fig. 5B, D). The higher the cell density, the earlier
168 the bud emerged (Fig. 5C). In contrast, the reported mode of division – fission followed
169 by budding – was predominantly observed when the cell density was high (Fig. 5B, E).
170 However, cells that formed buds without fission were also observed, which was not
171 reported in (Mitchison-Field et al., 2019) (Fig. 5B, F). The strain collected in (Mitchison-
172 Field et al., 2019) also showed filamentous growth at the lowest density in the liquid
173 culture (100%, n = 35). Thus, the division pattern variability of *H. werneckii* was similar
174 to that of *A. pullulans*. The finding corroborates the observation of the colonies on the
175 plate for >30 *H. werneckii* strains, where both filamentous and yeast-like cells are
176 identified (Zalar et al., 2019).

178 **Cell density-dependent division pattern alteration in an unidentified black yeast species**

179 In the present study, another yeast strain (NU30) formed dark brown-coloured colonies
180 on the plate (Fig. 6A). The barcode sequences did not perfectly match any registered
181 species; because the mismatch was large, the name of this yeast could not be determined.
182 To reveal its growth/division pattern and test if it was altered depending on the initial cell
183 density, time-lapse imaging was conducted at four different initial cell densities ($\times 1$, $\times 10$,
184 $\times 100$, and $\times 700$). The cell division pattern observed was remarkably similar to that of *H.*
185
186

187 *werneckii* (Fig. 6B–F, Video 5). Budding occurred after multiple septations when the
188 initial cell density was low, whereas a mother cell, without cell septation, produced
189 multiple buds sequentially from the same site (blue and magenta arrows) when the initial
190 cell density was high (Fig. 6E, F).

191 192 **Nuclear segregation scales with cell length in *H. werneckii***

193 In the model budding yeast *S. cerevisiae*, budding starts at the G1/S transition of the cell
194 cycle, and nuclear division takes place when the bud reaches a certain size (Juanes and
195 Piatti, 2016). In *S. pombe*, the nucleus is kept in the centre of the cell during interphase
196 (mostly G2 phase), then mitotic commitment occurs when the cell reaches a certain length
197 (~14 μm) (Wood and Nurse, 2015). In both cases, cell division (septation) occurs
198 immediately after nuclear division, producing daughter cells that have an identical shape
199 to the mother. In contrast, in *A. nidulans* and *Ashbya gossypii*, the model filamentous
200 fungi, multiple nuclear divisions take place without septation in the tip-growing cells,
201 resulting in the production of multinucleated cells (Fischer, 1999; Gladfelter et al., 2006).
202 It was curious whether nuclear and cell divisions were coupled in the above three black
203 yeast species, whose division pattern was flexible.

204 To follow nuclear division and septation/budding in live cells, their nuclei were
205 stained with Hoechst 33342, which is known to be permeable in many cell types,
206 including *S. pombe* (Haraguchi et al., 1999). However, staining and live imaging of *A.*
207 *pullulans* and NU30 were not successful. In contrast, *H. werneckii* was stainable, and its
208 nuclear dynamics was observable in real time (Fig. 7, Video 6, 7). Therefore, time-lapse
209 imaging with Hoechst 33342 using a spinning-disc confocal microscope was performed
210 for *H. werneckii*.

211 In the budding type of mitosis shown in Fig. 7A, which prevailed when the cell
212 density was high, nuclear separation occurred when the bud size reached 60 ± 11 % (\pm
213 SD) of the mother ($n = 30$). The nucleus was positioned in the mother, slightly on the bud
214 neck side at the time of chromosome condensation (i.e. mitotic entry) (44 ± 6 % position
215 from the bud neck). Sister chromatid separation occurred in the mother, and one of the
216 sister chromatids moved into the bud. Kymograph analysis indicated that the sister
217 chromatid motility relative to the cell edge was asymmetric (Fig. 7A, bottom): the sister
218 on the bud side moved much longer distances, whereas the sister in the mother moved
219 much less or sometimes showed bud-oriented movement. The maximum distance
220 between sister chromatids was 9.4 ± 1.1 μm , which was comparable to the mother cell
221 length (9.2 ± 1.0 μm) and was 36 % shorter than the entire cell length (i.e., daughter +
222 mother length). These results suggested that the anaphase spindle was motile in the cell.
223 The mitotic duration (chromosome condensation to anaphase onset) was 14 ± 7 min.
224 Septation, which was indicated by a straight line of the Hoechst dye at the bud neck, was
225 completed 16 ± 6 min after sister chromatid separation.

226 In the fission type of mitosis shown in Fig. 7B, the nucleus was positioned near the
227 centre of the cell at the time of chromosome condensation (16 or 24 out of 26 cells had
228 the nucleus at 45–55% or 40–60% position along the cell axis, respectively). After $16 \pm$
229 3 min ($n = 26$), the sister chromatids were separated. Unlike in *S. pombe*, chromosome
230 segregation did not always occur symmetrically (232–236 min time point in Video 6) and
231 the chromatids rarely reached the cell edge (maximum sister chromatid distance was 5.6
232 ± 0.5 μm , which was 54 ± 4 % of cell length) (Fig. 7B, bottom). Septation was completed
233 in the middle of the cell at 28 ± 4 min after sister chromatid separation.

234 In the tip-growing cells, which were observed at low cell density, a single nucleus
235 was detected, and it moved apically during tip growth, contrary to the multiple nuclei in
236 *A. nidulans* or *A. gossypii* (Fig. 7C and 7D; flare-like structures were also stained on the
237 cell surface by Hoechst 33342). Therefore, the nucleus stayed near the centre of the cell
238 (47 ± 5 % position from the tip at mitotic entry, $n = 32$). The cell length was quite variable
239 at the time of chromosome condensation (36 ± 11 μm , $\pm\text{SD}$, $n = 32$); in some cases, it
240 reached >40 μm , which was four times longer than the rod-shaped or budding cells
241 described above. Mitotic duration was 8.1 ± 1.2 min ($n = 27$). Sister chromatids moved
242 longer distances (53 ± 6 % of the cell length, $n = 31$) and septation occurred in the middle
243 of the two nuclei at 21 ± 3 min ($n = 26$) after sister chromatid separation. However, the
244 middle part was motile during anaphase, implying that the anaphase spindle was motile
245 in the cell. Consequently, the chromosome position at metaphase was not always
246 consistent with the septation position (Fig. 7D).

247 Thus, despite variations in cell size and geometry (rod, filament, bud), septation was
248 coupled with nuclear division. However, the segregating distance of sister chromatids
249 varied significantly, scaling with the cell length and shape. This suggests that the
250 mechanics of the cell division apparatus are adjusted to each mode of cell growth.

251 Discussion

252
253 Two major conclusions can be drawn from this study. First, a very limited local survey
254 has increased the list of marine-derived fungi, illustrating their diversity in the ocean. The
255 species could not be determined for several fungi, suggesting that they might represent
256 undescribed species. More comprehensive sampling and taxonomic analyses are needed
257 to further expand the list of fungi from the ocean.

258
259 Second, all three collected black yeast species changed their division mode
260 depending on the cell density. This plasticity may be beneficial for them, particularly
261 when they reside on the surfaces of animals and macroalgae. Filamentous growth with
262 branching is an excellent means to explore unoccupied areas (Coudert et al., 2019),
263 whereas budding in a crowded environment allows the clone to be released to the free
264 water and translocated to other animal/algae surfaces. This property somewhat resembles
265 that of filamentous fungi such as *Aspergillus*; they exhibited 2D hyphal growth, followed
266 by conidia (asexual spores) release (Adams et al., 1998). Switching between yeast-like
267 budding and hyphal growth is also observed for pathogenic, dimorphic fungi such as
268 *Candida albicans* (Merson-Davies and Odds, 1989; Sudbery et al., 2004; Sudbery, 2011).
269 However, the filament was curved and area exploration was not optimised for *H.*
270 *werneckii* and NU30; hence, the advantage of this growth/division mode remains unclear.

271 Combined with this and previous studies using live-cell microscopy (Mitchison-Field
272 et al., 2019), all five observed black yeast species showed at least two growth/division
273 patterns. The cell density-dependent plasticity might lie in nutritional states. For example,
274 some *H. werneckii* strains show different morphology on the plate depending on the
275 presence or absence of NaCl in the medium (Zalar et al., 2019). Alternatively, a quorum-
276 sensing mechanism (Albuquerque and Casadevall, 2012) might be responsible for the
277 inhibition of filament formation at high cell densities. Elucidating the chemical and/or
278 physical cues that trigger the division mode alteration and the prevalence of plasticity in
279 marine fungi would be interesting topics for future research.

281 **Materials and methods**

282

283 *Isolation of marine fungi at NU-MBL*

284 Samples were collected for 8 days from 4th March to 5th June 2020, in which the majority
 285 were obtained on the 22nd and 23rd of April. The ocean water temperature was 15.5 °C
 286 and the salinity was 34.9 ‰. This salinity indicates that there was no significant fresh
 287 water flow into this area from the large rivers in Ise Bay. Surface water samples were
 288 collected at the pier of the NU-MBL using a plastic bucket (Lat. 34°29'8"N, Long.
 289 136°52'32"E) (Fig. 1B, green). One litre of seawater was filtered using a 0.45-µm
 290 Millipore Stericup to obtain a 100× concentration. One millilitre of the concentrate was
 291 spread onto three types of media, which were similar to those used in (Mitchison-Field et
 292 al., 2019): YPD (10 g/L yeast extract, 10 g/L peptone [Bacto tryptone], 20 g/L glucose,
 293 12 g/L agar in seawater), malt medium (20 g/L malt extract, 6 g/L tryptone, 20 g/L glucose,
 294 12 g/L agar in seawater), and potato dextrose (24 g/L potato dextrose broth, 12 g/L agar
 295 in seawater). All species tested could grow on any medium; retrospectively, the
 296 preparation of three different media was not needed. Sediment samples were collected
 297 once by taking the mud at the bottom of the outside tank (Fig. 1C). Seaweeds were
 298 collected from the intertidal zone in front of the NU-MBL (Fig. 1B, magenta).
 299 Approximately 3 cm × 3 cm fragments of seaweed were obtained, which were rinsed with
 300 semi-sterile seawater (~500 mL) three times, followed by knife-cutting into small pieces
 301 and spreading onto a plate (Fig. 1D). All media were made with seawater at NU-MBL,
 302 which was pre-filtered with ADVANTEC filter paper #2. Antibiotics were added to the
 303 medium to avoid bacterial growth (20 µg/mL carbenicillin, 100 µg/mL chloramphenicol,
 304 10 µg/mL tetracycline) (Mitchison-Field et al., 2019). All fungal isolates were stored at -
 305 80 °C in YPD medium containing 20% glycerol.

306

307 *PCR and sequencing*

308 The ITS and NL sequences were sequenced for all strains using the primers listed in Table
 309 1. If the species could not be determined through these two sequences, other loci were
 310 amplified and sequenced (Rpb2, actin, calmodulin, EF1α, β-tubulin). PCR was performed
 311 with the KOD-ONE kit (TOYOBO) using a colony or the extracted genomic DNA as the
 312 template. DNA extraction was performed by boiling a piece of fungal colony for 5 min
 313 in 0.25% SDS followed by table-top centrifugation.

314

315 **Table 1: Primers used in this study**

Locus	Primer ID	Primer sequences	References
ITS1/4	7577-ITS1 (fungi)	TCCGTAGGTGAACCTGCGG	(White et al., 1990)
	7578-ITS4 (fungi)	TCCTCCGCTTATTGATATGC	
NL1/4	7579-NL1 (fungi)	GCATATCAATAAGCGGAGGAAAAG	(Kurtzman and Robnett, 1998)
	7580-NL4 (fungi)	GGTCCGTGTTTCAAGACGG	
Rpb2	7603-RPB-PenR1	GTTACACDCAACTYGTGCGYGA	(Manitchotpisit et al., 2009)
	7604-RPB-PenR2	GGCAGGGTGAATYTCGCAATG	
Actin	7774-ACT-512F	ATGTGCAAGGCCGTTTCGC	(Carbone and Kohn, 2019)
	7775-ACT-783R	TACGAGTCCTTCTGGCCCAT	
Calmodulin	7770-CMD5	CCGAGTACAAGGARGCCTTC	(Hong et al., 2006)
	7771-CMD6	CCGATRGAGGTACATRACGTGG	

EF1 α	7776-EF1-983F	GCYCCYGGHCAYCGTGAYTTYAT	(Rehner, 2001)
	7777-EF1-2218R	ATGACACCACRGCRCACRGTYTG	
β -Tubulin	7607-fungal-b-tub-Fw1	CGTGACAGGGTAACCAAATTGGTG	
	7608-fungal-b-tub-Fw2	GAGCCCGGTACCATGGACG	
	7609-fungal-b-tub-Rv1	GGTGATCTGGAAACCCTGGAGG	
	7610-fungal-b-tub-Rv2	CCCATAACCGGCACCGGTACC	

316

317 *Species identification*

318 Sequence homology was determined using the BLASTN program. If both ITS and NL
319 sequences were perfectly matched to a single species, the fungal isolate was concluded to
320 be the species. In some cases, either the ITS or NL sequences had a 100% match to a
321 certain species, whereas the other did not show an exact match. When the mismatch was
322 less than 3 bp, the fungal isolate was likely the species with a slight strain-specific
323 sequence variation, whereas a >3 bp mismatch in two or three barcodes led to the
324 assignment of possible novel species or genera. If a species could not be specified with
325 ITS and NL, the sequences of β -tubulin, Rpd2, actin, calmodulin, and EF1 α were also
326 used, dependent on the genus. For example, when ITS and NLS sequences perfectly
327 matched several *Cladosporium* species, the actin locus was further sequences and
328 specified the species. Calmodulin sequences were used for *Penicillium*. All the barcode
329 sequences are presented in Table S1.

330

331 *Live microscopy*

332 Initially, cells grown on the YPD plate were directly inoculated into YPD liquid medium
333 in an 8-well glass-bottom dish (Iwaki). However, the division modes were not consistent
334 between experiments for some species. Therefore, cells were grown in a YPD liquid
335 medium until saturation and inoculated into an 8-well plate after cell counting (300 μ L
336 culture volume). Note that this liquid-based imaging condition is different from that in
337 (Mitchison-Field et al., 2019), in which agar pads were used. The growths of 10^3 , 10^4 ,
338 10^5 , and $>10^5$ cells were compared for black yeasts. Transmission light imaging was
339 carried out at 23 °C with a Nikon inverted microscope (Ti) with a 40 \times 0.95 NA lens (Plan
340 Apo) and a Zyla CMOS camera (Andor). The brightness and contrast of the obtained
341 images were adjusted using FIJI software. The statistical analyses were performed using
342 the GraphPad Prism software. For DNA imaging of *Hortaea werneckii*, cells were
343 cultured with a more transparent medium. Synthetic minimal medium, similar to what
344 was used for *Aspergillus nidulans*, was made with seawater (6 g/L NaNO₃, 0.52 g/L KCl,
345 1.52 g/L KH₂PO₄, 10 g/L glucose, 1.5 mL trace elements, 10 mg/L biotin, 0.25 g/L
346 MgSO₄, pH = 6.5 [adjusted with NaOH]) (Edzuka et al., 2014). Hoechst 33342 was added
347 at 3–6 μ g/mL (final). DNA imaging was performed with another Nikon inverted
348 microscope (Ti2) attached to a 100 \times 1.40 NA lens, a 405-nm laser, CSU-10 spinning-disc
349 confocal unit, and the CMOS camera Zyla (at 23 °C). The time intervals used were mostly
350 2 min, but sometimes 2.5 min or 5 min was used. The microscopes were controlled using
351 NIS Elements software (Nikon).

352

353 **Acknowledgements**

354 I am grateful to Tomoya Edzuka and Maki Shirae-Kurabayashi for seaweed collection,
355 Masahiro Suzuki (Kobe University) for help with seaweed identification, Masashi
356 Fukuoka for daily temperature and salinity measurements, Naoto Jimi for helpful

357 comments on taxonomy, Amy Gladfelter (Marine Biological Laboratory, Woods
358 Hole/University of North Carolina) and Christine Field (Marine Biological Laboratory,
359 Woods Hole/Harvard Medical School) for yeast strains, and Amy Gladfelter for the
360 introduction to marine fungal biology and encouraging sample collection on the Japanese
361 coast. This work was supported by JSPS KAKENHI (17H06471, 18KK0202).
362

363 **Table 2. List of marine fungi identified in this study (alphabetical order)**




ID	Species	Site	Collection type	*1	*2
NU15	<i>Alternaria chlamydospora</i>	outdoor tank	Bryopsis		n.d.
NU14	<i>Arthopyrenia salicis</i>	rope at pier	Ulva		n.d.
NU29	<i>Arthrimum arundinis</i>	outdoor tank	surface water		n.d.
NU11	<i>Aspergillus protuberus</i>	rope at pier	Undaria		n.d.
NU47	<i>Aspergillus tabacinus</i>	intertidal zone	Lomentaria		n.d.
NU33	<i>Aspergillus versicolor</i>	water at pier tip	surface water		n.d.
NU41	<i>Aspergillus westerdijkiae</i>	intertidal zone	Undaria		n.d.
NU67	<i>Aureobasidium pullulans</i>	water at pier tip	surface water		
NU45	<i>Candida sake</i>	intertidal zone	Codium		
NU26	<i>Cladosporium cladosporioides</i>	outdoor tank	surface water		n.d.
NU56	<i>Cladosporium halotolerans</i>	intertidal zone	Lomentaria		n.d.
NU4	<i>Cladosporium perangustum</i>	outdoor tank	sediment		n.d.
NU22	<i>Cladosporium pseudocladosporioides</i>	outdoor tank	surface water		n.d.
NU19	<i>Cladosporium rectoides</i>	outdoor tank	surface water		n.d.
NU13	<i>Cladosporium sp.</i>	outdoor tank	Codium		n.d.
NU34	<i>Cladosporium tenuissimum</i>	intertidal zone	Lomentaria		n.d.
NU6	<i>Cystobasidium slooffiae</i>	rope at pier	Undaria		
NU59	<i>Diaporthe sp.</i>	intertidal zone	Spatoglossum		n.d.
NU40	<i>Didymella heteroderae</i>	intertidal zone	Ulva		n.d.
NU64	<i>Didymella sp.</i>	intertidal zone	Codium		n.d.
NU39	<i>Epicoccum laticollum (or E. sorghinum)</i>	intertidal zone	Champia		n.d.
NU49	<i>Filobasidium magnum</i>	intertidal zone	Ulva		
NU24	<i>Filobasidium sp.</i>	outdoor tank	surface water		
NU37	<i>Fusarium incarnatum</i>	intertidal zone	Champia		n.d.
NU28	<i>Hortaea werneckii</i>	outdoor tank	surface water		
NU32	<i>Hortaea werneckii</i>	water at pier tip	surface water		
NU2	<i>Kluyveromyces nonfermentans</i>	outdoor tank	sediment		
NU42	<i>Letendraea sp.(1)</i>	intertidal zone	Undaria		n.d.
NU54	<i>Letendraea sp.(2)</i>	intertidal zone	Codium		n.d.

NU61	<i>Leucosporidium intermedium</i>	intertidal zone	Undaria		
NU27	<i>Metschnikowia bicuspidata</i>	outdoor tank	surface water		
NU73	<i>Meyerozyma guilliermondii</i>	water at pier tip	surface water		
NU69	<i>Microdochium</i> sp.	water at pier tip	surface water		n.d.
NU65	<i>Neoscochyta paspali</i>	intertidal zone	Laurencia-like		n.d.
NU46	<i>Neopestalotiopsis clavispora</i>	intertidal zone	Lomentaria		n.d.
NU48	<i>Neopestalotiopsis</i> sp.	intertidal zone	Champia		n.d.
NU21	<i>Paraboeremia putaminum</i>	outdoor tank	surface water		n.d.
NU57	<i>Paradendryphiella arenariae</i>	intertidal zone	Champia		n.d.
NU18	<i>Parengyodontium album</i>	outdoor tank	Dasya		n.d.
NU36	<i>Penicillium brasilianum</i>	intertidal zone	Grateloupia		n.d.
NU38	<i>Penicillium brevicompactum</i>	intertidal zone	Champia		n.d.
NU52	<i>Penicillium janczewskii</i>	intertidal zone	Fushitsunagia		n.d.
NU20	<i>Penicillium citrinum</i>	outdoor tank	surface water		n.d.
NU5	<i>Penicillium concentricum</i>	outdoor tank	sediment		n.d.
NU71	<i>Penicillium glandicola</i>	intertidal zone	Colpomenia		n.d.
NU55	<i>Penicillium lenticrescens</i>	intertidal zone	Laurencia-like		n.d.
NU51	<i>Penicillium magnielliptisporum</i>	intertidal zone	Fushitsunagia		n.d.
NU3	<i>Penicillium marinum</i>	outdoor tank	sediment		n.d.
NU53	<i>Penicillium</i> sp.	intertidal zone	Colpomenia		n.d.
NU62	<i>Penicillium</i> sp. (or <i>P. alogum</i>)	intertidal zone	Fushitsunagia		n.d.
NU44	<i>Pestalotiopsis portugalia</i>	intertidal zone	Colpomenia		n.d.
NU1	<i>Pestalotiopsis</i> sp.	outdoor tank	sediment		n.d.
NU25	<i>Phacidium</i> sp.	outdoor tank	surface water		n.d.
NU43	<i>Phoma moricola</i>	intertidal zone	Fushitsunagia		n.d.
NU35	<i>Pseudopithomyces chartarum</i>	intertidal zone	Lomentaria		n.d.
NU50	<i>Pyrenochaetopsis</i> sp.	intertidal zone	Undaria		n.d.
NU68	<i>Rhodotorula babjevae</i> (or <i>R. glutinis</i>)	water at pier tip	surface water		
NU17	<i>Simplicillium lanosoniveum</i>	buoy at pier	Polysiphonia OR Melanothamnus		n.d.
NU58	<i>Sphaerulina rhabdoclinis</i>	intertidal zone	Champia		
NU70	<i>Sphaerulina</i> sp.	intertidal zone	Fushitsunagia		





NU72	<i>Trichoderma atroviride</i>	intertidal zone	Spatoglossum		n.d.
NU23	<i>Umbelopsis isabellina</i>	outdoor tank	surface water		n.d.
NU31	<i>Ustilago sp.</i>	outdoor tank	surface water		
NU63	Unclear	intertidal zone	Colpomenia		n.d.
NU30	Unclear	outdoor tank	surface water		
NU74	Unclear	water at pier tip	surface water		n.d.

364
365

***1 Comparison with the fungal list of Mitchison-Field et al. (2019)**

	same species identified
	same genus, but not species, identified
	unidentified genus

***2 Division type**

	budding, site fixed
	budding, site variable
	density-dependent
	multiple fissions
	rod shaped, budding

366

367 **References**

368

369 Adams, T.H., J.K. Wieser, and J.H. Yu. 1998. Asexual sporulation in *Aspergillus*
370 *nidulans*. *Microbiol Mol Biol Rev.* 62:35-54.

371 Albuquerque, P., and A. Casadevall. 2012. Quorum sensing in fungi--a review. *Med*
372 *Mycol.* 50:337-345.

373 Amend, A., G. Burgaud, M. Cunliffe, V.P. Edgcomb, C.L. Ettinger, M.H. Gutierrez, J.
374 Heitman, E.F.Y. Hom, G. Ianiri, A.C. Jones, M. Kagami, K.T. Picard, C.A.
375 Quandt, S. Raghukumar, M. Riquelme, J. Stajich, J. Vargas-Muniz, A.K. Walker,
376 O. Yarden, and A.S. Gladfelter. 2019. Fungi in the Marine Environment: Open
377 Questions and Unsolved Problems. *mBio.* 10.

378 Carbone, I., and L.M. Kohn. 2019. A method for designing primer sets for speciation
379 studies in filamentous ascomycetes. *Mycologia.* 91:553-556.

380 Coudert, Y., S. Harris, and B. Charrier. 2019. Design Principles of Branching
381 Morphogenesis in Filamentous Organisms. *Curr Biol.* 29:R1149-R1162.

382 Edzuka, T., L. Yamada, K. Kanamaru, H. Sawada, and G. Goshima. 2014. Identification
383 of the augmin complex in the filamentous fungus *Aspergillus nidulans*. *PLoS One.*
384 9:e101471.

385 Feyder, S., J.O. De Craene, S. Bar, D.L. Bertazzi, and S. Friant. 2015. Membrane
386 trafficking in the yeast *Saccharomyces cerevisiae* model. *Int J Mol Sci.* 16:1509-
387 1525.

388 Fischer, R. 1999. Nuclear movement in filamentous fungi. *FEMS Microbiol Rev.* 23:39-
389 68.

390 Gladfelter, A.S., A.K. Hungerbuehler, and P. Philippsen. 2006. Asynchronous nuclear
391 division cycles in multinucleated cells. *J Cell Biol.* 172:347-362.

392 Gladfelter, A.S., T.Y. James, and A.S. Amend. 2019. Marine fungi. *Curr Biol.* 29:R191-
393 R195.

394 Gostincar, C., L. Muggia, and M. Grube. 2012. Polyextremotolerant black fungi:
395 oligotrophism, adaptive potential, and a link to lichen symbioses. *Front Microbiol.*
396 3:390.

397 Haraguchi, T., D.Q. Ding, A. Yamamoto, T. Kaneda, T. Koujin, and Y. Hiraoka. 1999.
398 Multiple-color fluorescence imaging of chromosomes and microtubules in living
399 cells. *Cell Struct Funct.* 24:291-298.

400 Hong, S.B., H.S. Cho, H.D. Shin, J.C. Frisvad, and R.A. Samson. 2006. Novel
401 *Neosartorya* species isolated from soil in Korea. *Int J Syst Evol Microbiol.* 56:477-
402 486.

403 Juanes, M.A., and S. Piatti. 2016. The final cut: cell polarity meets cytokinesis at the bud
404 neck in *S. cerevisiae*. *Cell Mol Life Sci.* 73:3115-3136.

405 Kopecka, M., M. Gabriel, K. Takeo, M. Yamaguchi, A. Svoboda, and K. Hata. 2003.
406 Analysis of microtubules and F-actin structures in hyphae and conidia
407 development of the opportunistic human pathogenic black yeast *Aureobasidium*
408 *pullulans*. *Microbiology (Reading).* 149:865-876.

409 Kurtzman, C.P., and C.J. Robnett. 1998. Identification and phylogeny of ascomycetous
410 yeasts from analysis of nuclear large subunit (26S) ribosomal DNA partial
411 sequences. *Antonie Van Leeuwenhoek.* 73:331-371.

412 Manitchotpisit, P., T.D. Leathers, S.W. Peterson, C.P. Kurtzman, X.L. Li, D.E. Eveleigh,
413 P. Lotrakul, S. Prasongsuk, C.A. Dunlap, K.E. Vermillion, and H. Punnapayak.

414 2009. Multilocus phylogenetic analyses, pullulan production and xylanase
415 activity of tropical isolates of *Aureobasidium pullulans*. *Mycol Res.* 113:1107-
416 1120.

417 Merson-Davies, L.A., and F.C. Odds. 1989. A morphology index for characterization of
418 cell shape in *Candida albicans*. *J Gen Microbiol.* 135:3143-3152.

419 Mitchison-Field, L.M.Y., J.M. Vargas-Muniz, B.M. Stormo, E.J.D. Vogt, S. Van
420 Dierdonck, J.F. Pelletier, C. Ehrlich, D.J. Lew, C.M. Field, and A.S. Gladfelter.
421 2019. Unconventional Cell Division Cycles from Marine-Derived Yeasts. *Curr*
422 *Biol.* 29:3439-3456 e3435.

423 Moreno, L.F., V.A. Vicente, and S. de Hoog. 2018. Black yeasts in the omics era:
424 Achievements and challenges. *Med Mycol.* 56:32-41.

425 Nurse, P., and J. Hayles. 2019. Using genetics to understand biology. *Heredity (Edinb).*
426 123:4-13.

427 OBIS. <https://obis.org/>. ocean biodiversity information system.

428 Osmani, S.A., and P.M. Mirabito. 2004. The early impact of genetics on our
429 understanding of cell cycle regulation in *Aspergillus nidulans*. *Fungal Genet Biol.*
430 41:401-410.

431 Rehner, S. 2001. Primers for Elongation Factor 1-a(EF1-a). [http://](http://ocid.nacse.org/research/deephyphae/EF1primer.pdf)
432 ocid.nacse.org/research/deephyphae/EF1primer.pdf.

433 Sudbery, P., N. Gow, and J. Berman. 2004. The distinct morphogenic states of *Candida*
434 *albicans*. *Trends Microbiol.* 12:317-324.

435 Sudbery, P.E. 2011. Growth of *Candida albicans* hyphae. *Nat Rev Microbiol.* 9:737-748.

436 White, T.J., T. Bruns, S. Lee, and J.W. Taylor. 1990. Amplification and direct sequencing
437 of fungal ribosomal RNA Genes for phylogenetics. In Innis, M. A., Gelfand, D.
438 H., Sninsky, J. J. & White, T. J. (eds.), PCR Protocols: A Guide to Methods and
439 Applications. *Academic Press*:315-322.

440 Wood, E., and P. Nurse. 2015. Sizing up to divide: mitotic cell-size control in fission
441 yeast. *Annu Rev Cell Dev Biol.* 31:11-29.

442 Zalar, P., J. Zupancic, C. Gostincar, J. Zajc, G.S. de Hoog, F. De Leo, A. Azua-Bustos,
443 and N. Gunde-Cimerman. 2019. The extremely halotolerant black yeast *Hortaea*
444 *werneckii* - a model for intraspecific hybridization in clonal fungi. *IMA Fungus.*
445 10:10.

446
447
448 **Figure legends**

449
450 **Figure 1. Collection of marine fungi from surface ocean water, sediment, and**
451 **seaweeds**

452 (A) Location of Sugashima Marine Biological Laboratory (NU-MBL). (B) Surface ocean
453 water was obtained at the pier (green), whereas seaweeds were collected at the intertidal
454 zone (magenta). (C) Outdoor tank at NU-MBL which has a continuous flow of unfiltered
455 sea water. The sediment and surface water were the sources of marine fungi. (D) Severed
456 seaweeds on the fungal medium plate. Several fungal colonies grew after several days.
457 (E) Examples of fungal colonies on the plate (sediment sample). Each colony was marked
458 and subjected to genotyping PCR and transfer to a fresh plate.

459
460 **Figure 2. Examples of fungal colonies**

461 Fifteen fungal colonies, whose identity could not be determined, are shown. Filamentous
462 fungi were inoculated onto the centre of the YPD plate, whereas yeasts were streaked.
463 They were incubated at 18°C for indicated days. The diameter of the plates in this figure
464 is 9 cm.

465

466 **Figure 3. Budding yeast has either a fixed or variable budding site**

467 (A) *S. cerevisiae*-type budding yeast, where a bud emerges at seemingly random sites on
468 the round mother cell. (B) The budding site is fixed at one site of the mother cell. Blue
469 arrows, initially emerged bud; magenta arrow, second bud; green arrow, third bud. Scale
470 bars, 10 µm.

471

472 **Figure 4. Division pattern variation in the black yeast *Aureobasidium pullulans***

473 (A) *A. pullulans* colonies. The peripheries of the colonies turned brown after prolonged
474 storage at 4 °C (fresh colonies are uncoloured). (B) Four distinct bud formation patterns
475 dependent on the initial cell density. Saturated cultures were diluted at four different
476 concentrations, and the growth and budding style was assessed (n = 22, 18, 25, 30 [left to
477 right]). (C) Timing of bud emergence after a cell started to grow in a filamentous manner
478 (± SEM) (n = 7, 18, 25, 11 [left to right]). The one-way ANOVA detected significant
479 differences between groups (F = 77.06, p < 0.0001). The post-hoc test was performed by
480 Tukey's test (p < 0.0001 for each comparison). (D) Filamentous growth with occasional
481 septation and branching, followed by budding from various sites on the filament. This
482 mode of growth/budding was dominant when the initial cell density was low. (E, F)
483 Immediate budding without apparent cell growth or septation. Two buds simultaneously
484 emerged at two opposite sites in (E), whereas two buds sequentially emerged at one site
485 of the mother cell in (F). Blue arrows, initially emerged buds; magenta arrow, second
486 bud; green, mother cell. Scale bars, 10 µm.

487

488 **Figure 5. Division pattern variation in the black yeast *Hortaea werneckii***

489 (A) Colonies of two *H. werneckii* strains, which had different growth rates. (B) Three
490 distinct bud formation patterns dependent on the initial cell density. Saturated cultures
491 were diluted at four different concentrations, and the growth and budding style was
492 assessed (n = 30, 11, 28, 54 [left to right]). (C) Timing of bud formation after the first
493 septation (± SEM) (n = 19, 11, 12 [left to right]). The one-way ANOVA detected
494 significant differences between three groups (F = 549.2, p < 0.0001). The post-hoc test
495 was performed by Tukey's test (p < 0.0001 for each comparison). (D) Filamentous growth
496 with septation and branching, followed by budding from various sites on the curved
497 filament (a released bud is seen at lower-left corner at 43 h). This mode of growth/budding
498 was dominant when the initial cell density was low. (E) Elongation, septation, followed
499 by budding. Multiple buds sequentially emerged from a "mother" cell that had undergone
500 septation. This mode of septation/budding was dominant when the initial cell density was
501 high. (F) Immediate budding without septation. Multiple buds sequentially emerged from
502 a "mother" cell. Blue and magenta arrows indicate the first and second buds, respectively.
503 Scale bars, 10 µm.

504

505 **Figure 6. Division pattern variation in an unidentified black yeast species "NU30"**

506 (A) Colonies of NU30. Each colony turned dark brown after prolonged storage at 4 °C
507 (fresh colonies were uncoloured). (B) Three distinct bud formation patterns dependent on

508 the initial cell density. Saturated cultures were diluted at four different concentrations,
509 and the growth and budding style was assessed (n = 25, 12, 25, 37 [left to right]). Asterisk:
510 the frequency of immediately budding cells was underestimated, as many cells did not
511 stick to the glass and were hard to count, whereas all the cells that underwent septations
512 were immobile and countable. (C) Timing of bud formation after the first septation (\pm
513 SEM) for the cells that formed multiple septations (n = 12, 12, 19 [left to right]). The one-
514 way ANOVA detected significant differences between groups (F = 811.7, p < 0.0001).
515 The post-hoc test was performed by Tukey's test (p < 0.0001 for each comparison). (D)
516 Filamentous growth with septation and branching, followed by budding from various sites
517 on the curved filament (20 h). This mode of growth/budding was dominant when the
518 initial cell density was low. (E) Single septation, followed by budding. Multiple buds
519 sequentially emerged from a "mother" cell that had undergone septation. (F) Immediate
520 budding without septation. Multiple buds sequentially emerged from the "mother" cell
521 (green). This mode of budding was dominant when the initial cell density was high. Blue
522 and magenta arrows indicate the first and second buds, respectively. Scale bars, 10 μ m.

523 **Figure 7. Nuclear dynamics in *H. werneckii***

524 (A) Nuclear dynamics during budding-type cell division. The corresponding kymograph
525 is shown at the bottom. Time 0 indicates mitotic entry. (B) Nuclear dynamics during
526 fission-type cell division. The corresponding kymograph is shown at the bottom. Time 0
527 indicates mitotic entry. (C, D) Nuclear dynamics in tip-growing cells. Green arrowheads,
528 interphase nuclei; magenta, position of condensed chromosomes at the mitotic entry; blue,
529 sister chromatids/nuclei; yellow, septum. Septum was formed at the site of mitotic
530 chromosomes in (C), whereas it was deviated in (D). Segregation of sister chromatids is
531 asymmetric relative to the metaphase chromosome.

532

533 **Supplementary video legends**

534

535 **Video 1. Cell division of marine-derived budding yeast**

536 Time-lapse imaging of two budding yeast species (5-min intervals). The budding site is
537 variable (left) or fixed (right) depending on the species.

538

539 **Video 2. Cell division of rod-shaped fungi *Ustilago* sp., *Leucosporidium intermedium*, 540 and *Sphaerulina rhabdoclinis***

541 Time-lapse imaging of three fungi that have a rod shape and form yeast-like colonies on
542 the plate (5-min interval).

543

544 **Video 3. Cell division of the black yeast *Aureobasidium pullulans***

545 Live imaging of *Aureobasidium pullulans* (NU67) at four different initial cell densities.
546 Images were acquired every 15 min.

547

548 **Video 4. Cell division of the black yeast *Hortaea werneckii***

549 Live imaging of *Hortaea werneckii* (NU28) at three different initial cell densities (lower
550 left, high: upper left, medium: right, low). Images were acquired every 15 min.

551

552 **Video 5. Cell division of an unidentified black yeast species**

553

554 Live imaging of NU30 (unnamed) at three different initial cell densities (lower left, high:
555 upper left, medium: right, low). Images were acquired every 15 min.

556

557 **Video 6. Nuclear dynamics in the black yeast *Hortaea werneckii* – budding and fission**

558 Live imaging of chromosomes in *Hortaea werneckii* (NU28) during budding- and fission-
559 type mitosis. Images were acquired every 2 min.

560

561 **Video 7. Nuclear dynamics in the black yeast *Hortaea werneckii* – growing tip**

562 Live imaging of chromosomes in *Hortaea werneckii* (NU28) during mitosis of tip-
563 growing cells. Images were acquired every 5 min. Note that flare-like structures are also
564 stained.

565

Figure 1

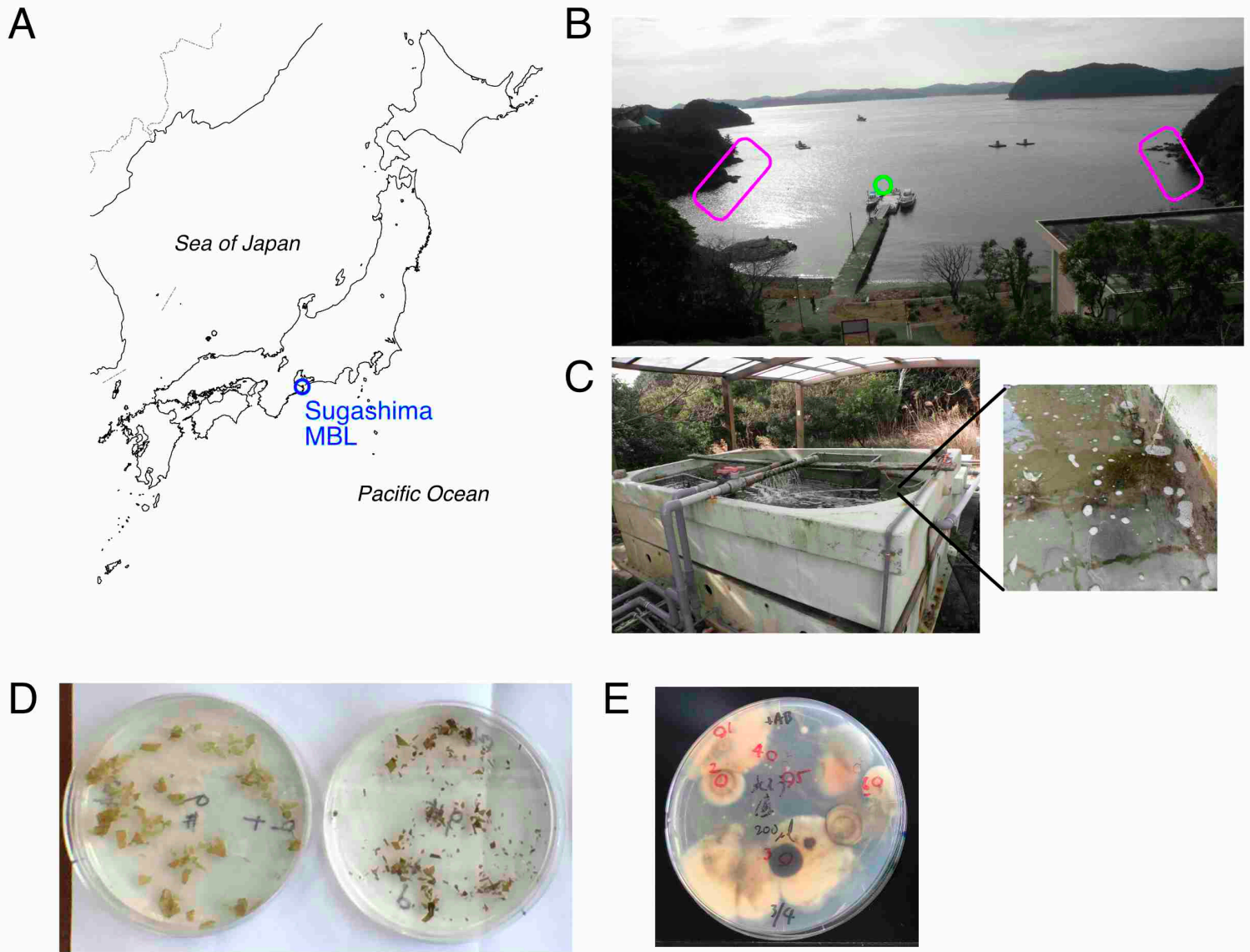


Figure 1. Collection of marine fungi from surface ocean water, sediment, and seaweeds

(A) Location of Sugashima Marine Biological Laboratory (NU-MBL). (B) Surface ocean water was obtained at the pier (green), whereas seaweeds were collected at the intertidal zone (magenta). (C) Outdoor tank at NU-MBL which has a continuous flow of unfiltered sea water. The sediment and surface water were the sources of marine fungi. (D) Severed seaweeds on the fungal medium plate. Several fungal colonies grew after several days. (E) Examples of fungal colonies on the plate (sediment sample). Each colony was marked and subjected to genotyping PCR and transfer to a fresh plate.

Figure 2

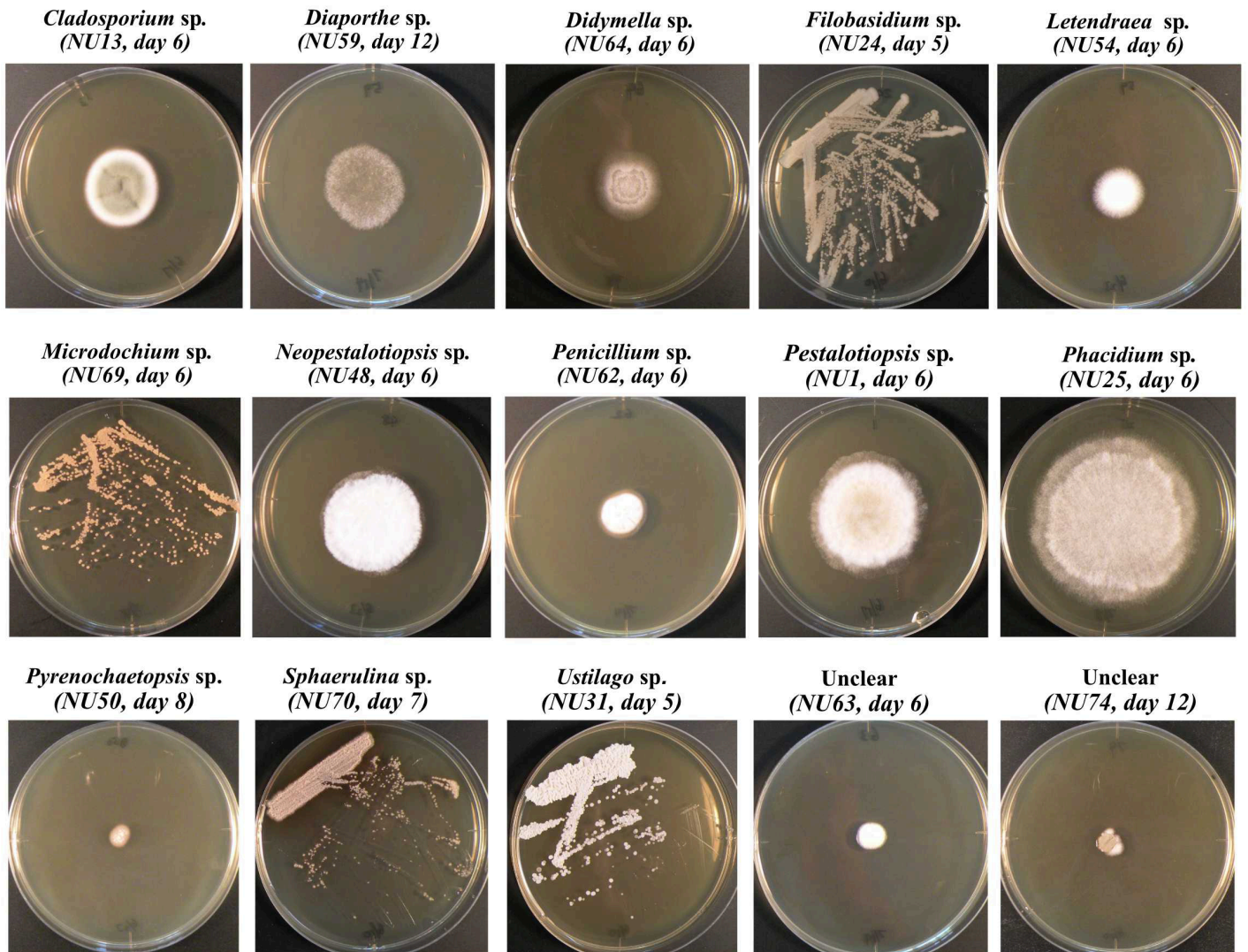
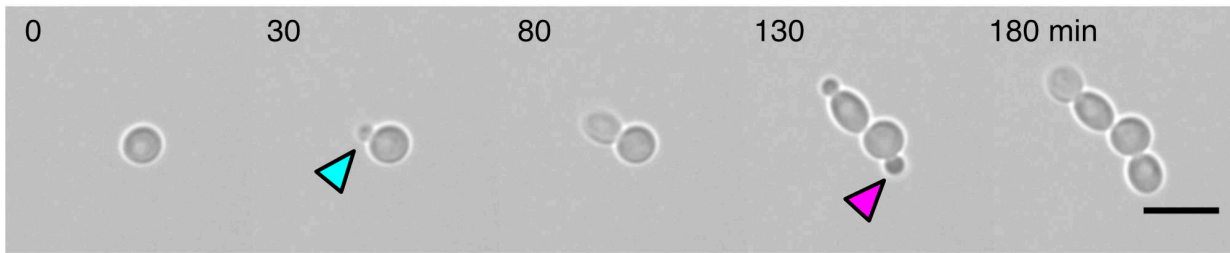


Figure 2. Examples of fungal colonies.

Fifteen fungal colonies, whose identity could not be determined, are shown. Filamentous fungi were inoculated onto the centre of the YPD plate, whereas yeasts were streaked. They were incubated at 18°C for indicated days. The diameter of the plates in this figure is 9 cm.

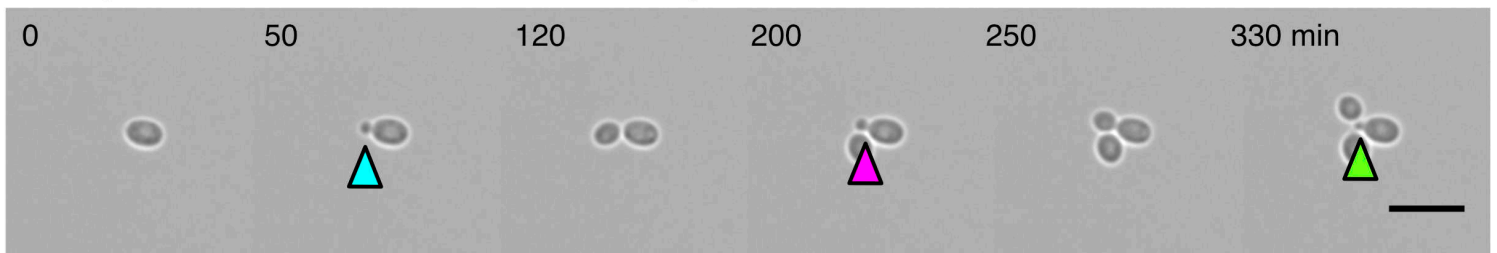
Figure 3

A *Metschnikowia bicuspidata* (variable budding site)



Others: *Candida sake*, *Kluyveromyces nonfermentans*, *Meyerozyma guilliermondii*, *Rhodotorula* sp.

B *Cystobasidium slooffiae* (fixed budding site)



Others: *Filobasidium magnum*, *Filobasidium* sp.

Figure 3. Budding yeast has either a fixed or variable budding site

(A) *S. cerevisiae*-type budding yeast, where a bud emerges at seemingly random sites on the round mother cell. (B) The budding site is fixed at one site of the mother cell. Blue arrows, initially emerged bud; magenta arrow, second bud; green arrow, third bud. Scale bars, 10 μ m.

Figure 4

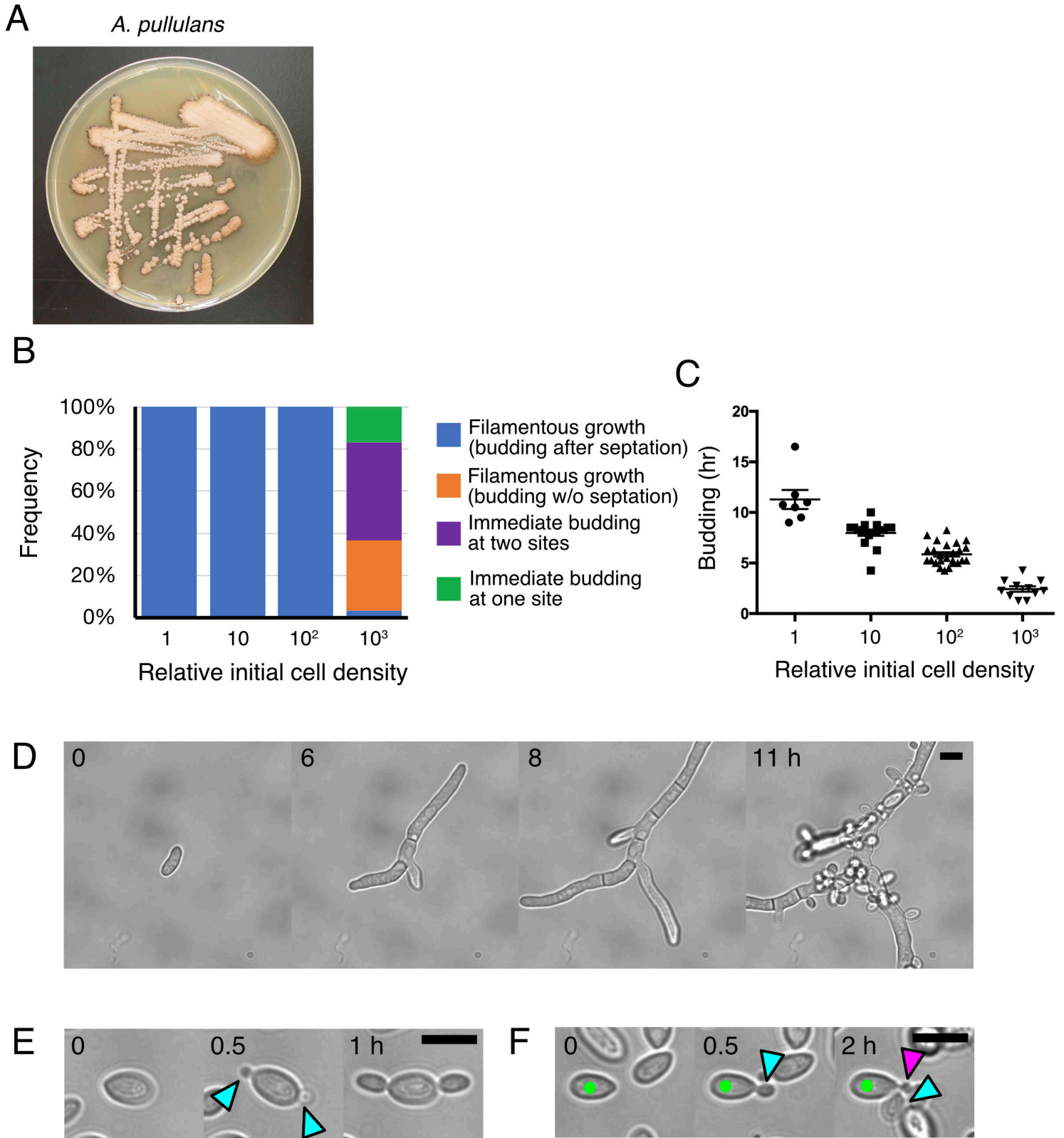


Figure 4. Division pattern variation in the black yeast *Aureobasidium pullulans*

(A) *A. pullulans* colonies. The peripheries of the colonies turned brown after prolonged storage at 4 °C (fresh colonies are uncoloured). (B) Four distinct bud formation patterns dependent on the initial cell density. Saturated cultures were diluted at four different concentrations, and the growth and budding style was assessed (n = 22, 18, 25, 30 [left to right]). (C) Timing of bud emergence after a cell started to grow in a filamentous manner (\pm SEM) (n = 7, 18, 25, 11 [left to right]). The one-way ANOVA detected significant differences between groups (F = 77.06, p < 0.0001). The post-hoc test was performed by Tukey's test (p < 0.0001 for each comparison). (D) Filamentous growth with occasional septation and branching, followed by budding from various sites on the filament. This mode of growth/budding was dominant when the initial cell density was low. (E, F) Immediate budding without apparent cell growth or septation. Two buds simultaneously emerged at two opposite sites in (E), whereas two buds sequentially emerged at one site of the mother cell in (F). Blue arrows, initially emerged buds; magenta arrow, second bud; green, mother cell. Scale bars, 10 μ m.

Figure 5

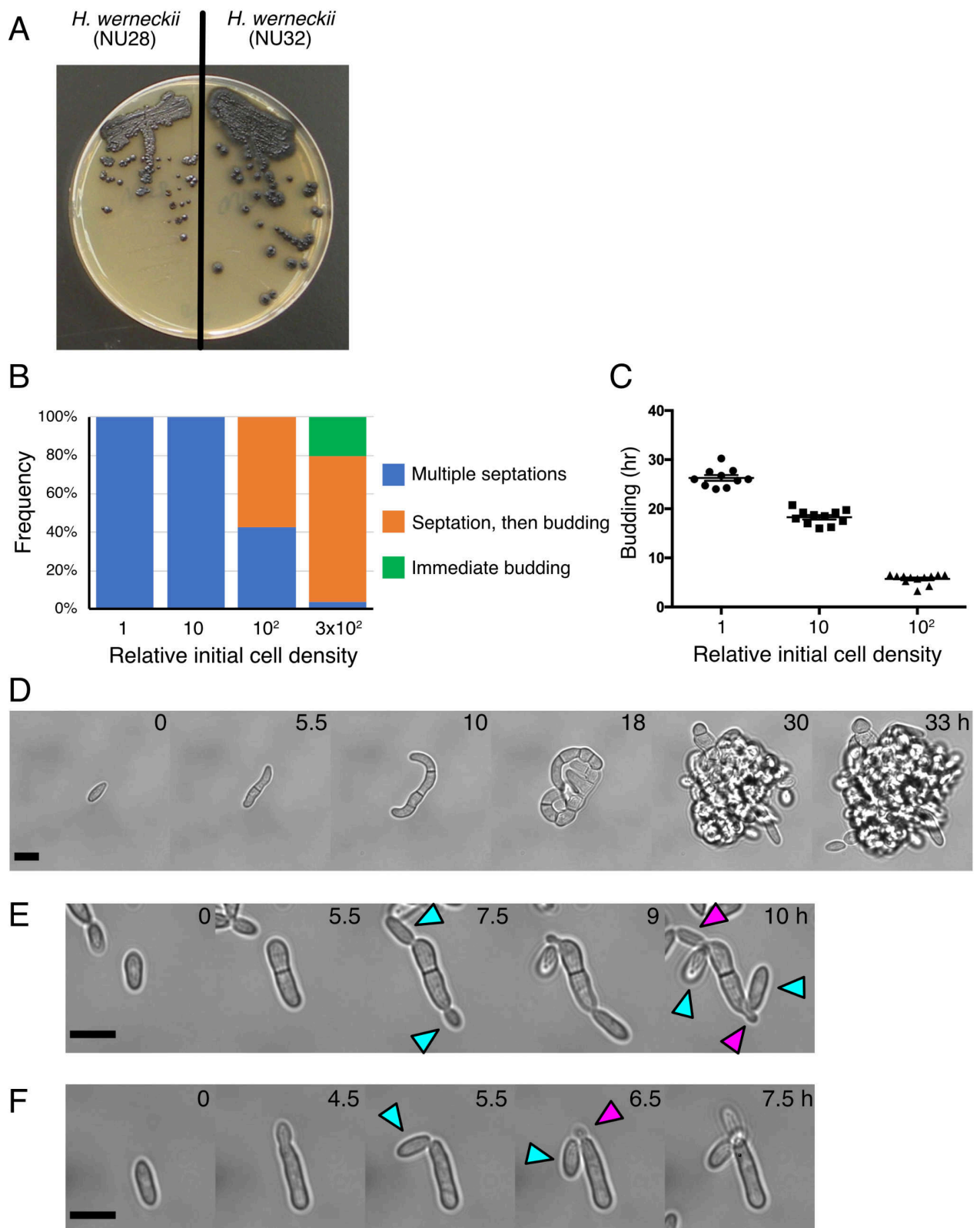


Figure 5. Division pattern variation in the black yeast *Hortaea werneckii*

(A) Colonies of two *H. werneckii* strains, which had different growth rates. (B) Three distinct bud formation patterns dependent on the initial cell density. Saturated cultures were diluted at four different concentrations, and the growth and budding style was assessed ($n = 30, 11, 28, 54$ [left to right]). (C) Timing of bud formation after the first septation (\pm SEM) ($n = 19, 11, 12$ [left to right]). The one-way ANOVA detected significant differences between three groups ($F = 549.2, p < 0.0001$). The post-hoc test was performed by Tukey's test ($p < 0.0001$ for each comparison). (D) Filamentous growth with septation and branching, followed by budding from various sites on the curved filament (a released bud is seen at lower-left corner at 43 h). This mode of growth/budding was dominant when the initial cell density was low. (E) Elongation, septation, followed by budding. Multiple buds sequentially emerged from a "mother" cell that had undergone septation. This mode of septation/budding was dominant when the initial cell density was high. (F) Immediate budding without septation. Multiple buds sequentially emerged from a "mother" cell. Blue and magenta arrows indicate the first and second buds, respectively. Scale bars, 10 μ m.

Figure 6

A *black yeast* "NU30"

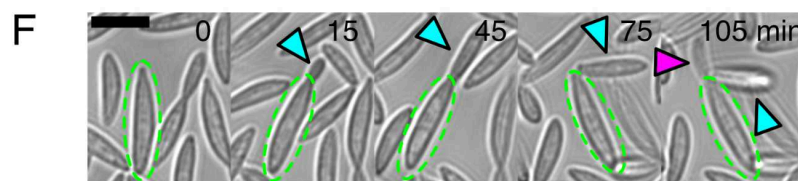
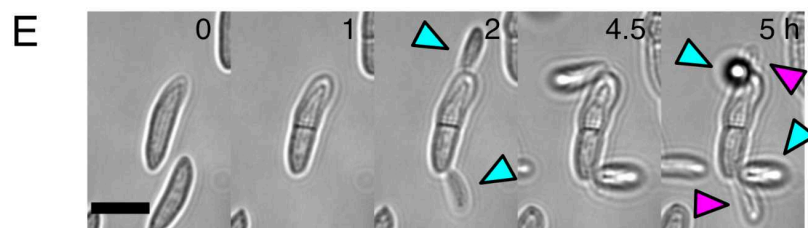
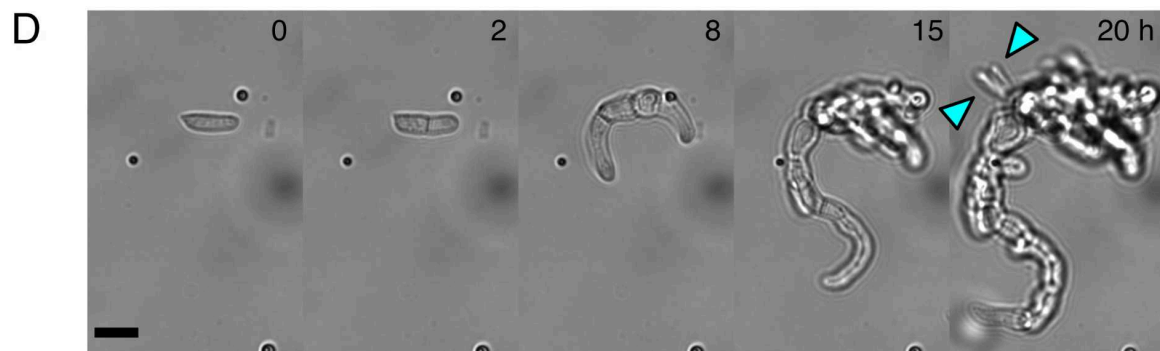
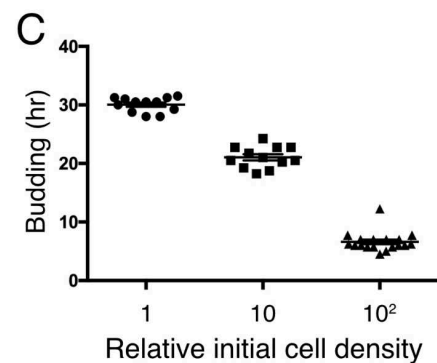
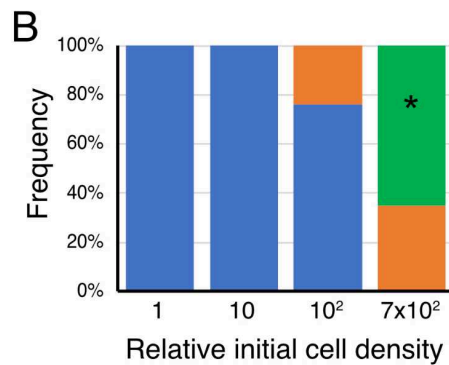


Figure 6. Division pattern variation in an unidentified black yeast species "NU30"

(A) Colonies of NU30. Each colony turned dark brown after prolonged storage at 4 °C (fresh colonies were uncoloured). (B) Three distinct bud formation patterns dependent on the initial cell density. Saturated cultures were diluted at four different concentrations, and the growth and budding style was assessed ($n = 25, 12, 25, 37$ [left to right]). Asterisk: the frequency of immediately budding cells was underestimated, as many cells did not stick to the glass and were hard to count, whereas all the cells that underwent septations were immobile and countable. (C) Timing of bud formation after the first septation (\pm SEM) for the cells that formed multiple septations ($n = 12, 12, 19$ [left to right]). The one-way ANOVA detected significant differences between groups ($F = 811.7, p < 0.0001$). The post-hoc test was performed by Tukey's test ($p < 0.0001$ for each comparison). (D) Filamentous growth with septation and branching, followed by budding from various sites on the curved filament (20 h). This mode of growth/budding was dominant when the initial cell density was low. (E) Single septation, followed by budding. Multiple buds sequentially emerged from a "mother" cell that had undergone septation. (F) Immediate budding without septation. Multiple buds sequentially emerged from the "mother" cell (green). This mode of budding was dominant when the initial cell density was high. Blue and magenta arrows indicate the first and second buds, respectively. Scale bars, 10 μm .

Figure 7

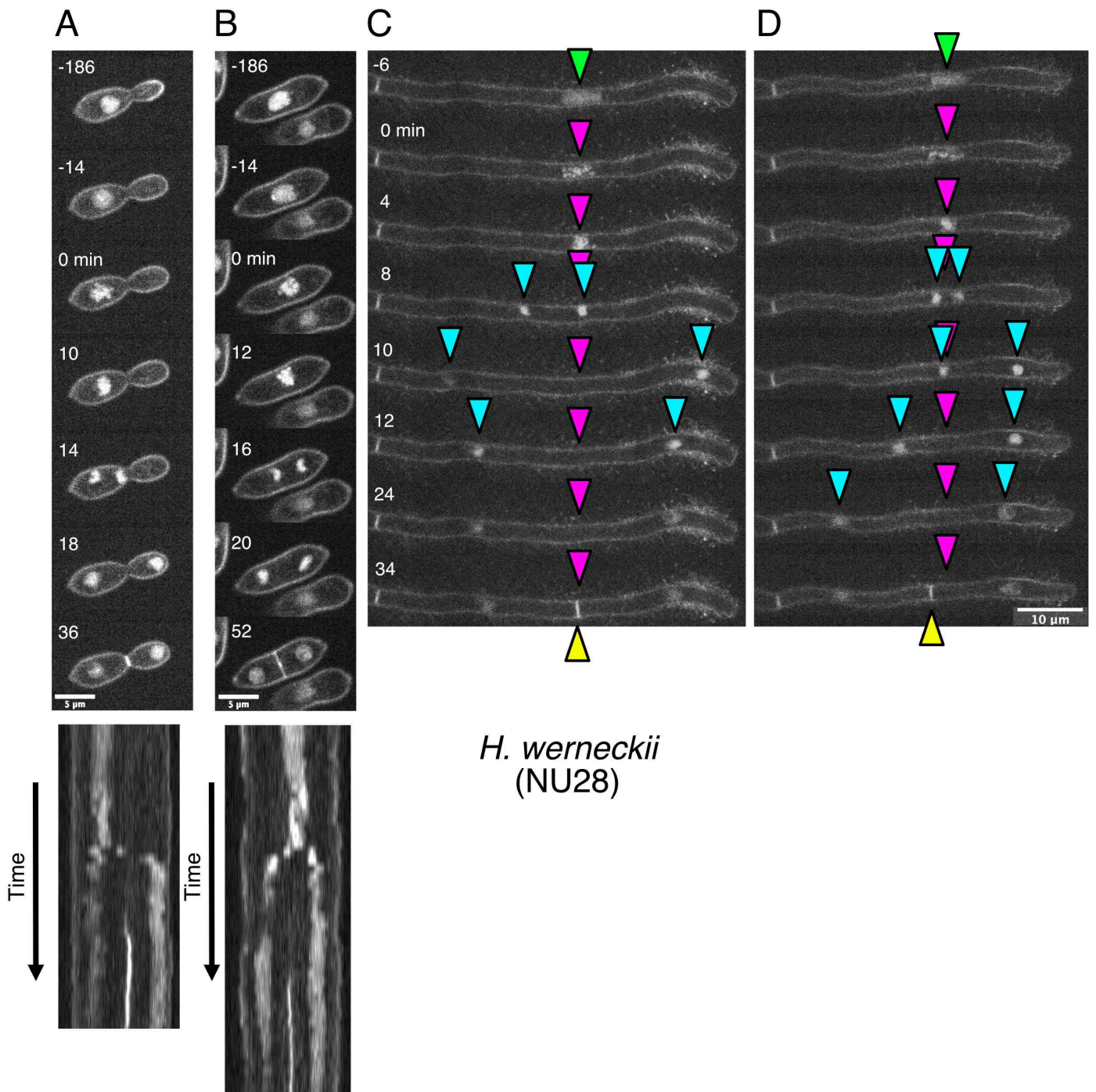


Figure 7. Nuclear dynamics in *H. werneckii*

(A) Nuclear dynamics during budding-type cell division. The corresponding kymograph is shown at the bottom. Time 0 indicates mitotic entry. (B) Nuclear dynamics during fission-type cell division. The corresponding kymograph is shown at the bottom. Time 0 indicates mitotic entry. (C, D) Nuclear dynamics in tip-growing cells. Green arrowheads, interphase nuclei; magenta, position of condensed chromosomes at the mitotic entry; blue, sister chromatids/nuclei; yellow, septum. Septum was formed at the site of mitotic chromosomes in (C), whereas it was deviated in (D). Segregation of sister chromatids is asymmetric relative to the metaphase chromosome.